Yes-associated protein (YAP) mediates adaptive cardiac hypertrophy in response to pressure overload

Received for publication, October 3, 2018, and in revised form, December 27, 2018 Published, Papers in Press, January 11, 2019, DOI 10.1074/jbc.RA118.006123

Jaemin Byun[‡1], Dominic P. Del Re[‡1], Peiyong Zhai[‡], Shohei Ikeda[‡], Akihiro Shirakabe[‡], Wataru Mizushima[‡], Shigeki Miyamoto[§], Joan H. Brown[§], and Junichi Sadoshima[‡2]

From the [‡]Department of Cell Biology and Molecular Medicine, Cardiovascular Research Institute, Rutgers-New Jersey Medical School, Newark, New Jersey 07103 and the [§]Department of Pharmacology, University of California San Diego, La Jolla, California 92093

Edited by Henrik G. Dohlman

Cardiovascular disease (CVD) remains the leading cause of death globally, and heart failure is a major component of CVD-related morbidity and mortality. The development of cardiac hypertrophy in response to hemodynamic overload is initially considered to be beneficial; however, this adaptive response is limited and, in the presence of prolonged stress, will transition to heart failure. Yes-associated protein (YAP), the central downstream effector of the Hippo signaling pathway, regulates proliferation and survival in mammalian cells. Our previous work demonstrated that cardiac-specific loss of YAP leads to increased cardiomyocyte (CM) apoptosis and impaired CM hypertrophy during chronic myocardial infarction (MI) in the mouse heart. Because of its documented cardioprotective effects, we sought to determine the importance of YAP in response to acute pressure overload (PO). Our results indicate that endogenous YAP is activated in the heart during acute PO. YAP activation that depended upon RhoA was also observed in CMs subjected to cyclic stretch. To examine the function of endogenous YAP during acute PO, $Yap^{+/flox};Cre^{\alpha\text{-}MHC}$ (YAP-CHKO) and $Yap^{+/flox}$ mice were subjected to transverse aortic constriction (TAC). We found that YAP-CHKO mice had attenuated cardiac hypertrophy and significant increases in CM apoptosis and fibrosis that correlated with worsened cardiac function after 1 week of TAC. Loss of CM YAP also impaired activation of the cardioprotective kinase Akt, which may underlie the YAP-CHKO phenotype. Together, these data indicate a prohypertrophic, prosurvival function of endogenous YAP and suggest a critical role for CM YAP in the adaptive response to acute PO.

Cardiovascular disease (CVD)[3] remains the leading cause of death globally, and heart failure is a major component of CVD-related morbidity and mortality (1). The development of cardiac hypertrophy in response to hemodynamic overload is considered initially beneficial, as it augments the number of contractile units and normalizes ventricular wall stress according to the Law of Laplace. Decreases in wall stress not only reduce oxygen consumption but also inhibit cell death (2). However, these adaptive responses have a limited capacity for protection and, in the presence of prolonged stress, will transition to heart failure (3). The heart also initiates additional adaptive mechanisms, including up-regulation of anti-oxidants and mitophagy, to cope with energetic stress, increased oxidative stress, and mitochondrial dysfunction (4). Yes-associated protein (YAP), a transcription cofactor and downstream effector of the Hippo pathway, regulates proliferation and survival in multiple cell types, including cardiomyocytes (CMs). We have shown that cardiac-specific loss of YAP in mice leads to increased CM apoptosis and a lethal dilated cardiomyopathy by 12 weeks of age. Heterozygous YAP depletion impaired hypertrophy and led to worsened heart function in response to volume overload imposed by chronic myocardial infarction (MI) in the mouse heart (5). However, the role of YAP in response to pressure overload (PO), another form of hemodynamic stress, has yet to be examined.

The etiologies of heart failure are divergent and include PO, ischemia, valvular disease, cardiomyopathy, and congenital heart disease (1). Among these, PO-related pathological cardiac hypertrophy is one of the most common causes of heart failure (6). Pathophysiologically, cardiac hypertrophy is an increase in the heart muscle mass resulting from increases in CM size together with proliferation of fibroblasts and increased deposition of extracellular matrix (7). Cardiac hypertrophy can initially be an adaptive response, serving to maintain cardiac function through reduction in wall stress and energy expenditure (8). However, insufficient accompanying growth/prolifer-

This work was supported by National Institutes of Health Grants HL127339 and HL135726 (to D. P. D.), HL097037 (to S. M.), HL080101, HL105242, and HL028143 (to J. H. B.), and HL067724, HL091469, HL112330, HL138720, and AG023039 (to J. S.), Tobacco-related Disease Research Program (TRDRP) Grant 26IP-0040 (to J. H. B.), the Foundation Leducq Transatlantic Network of Excellence 15CBD04 (to J. S.), and American Heart Association Grant 11SDG7240067 (to D. P. D.) and 15GRNTZ297009 (to S. M.). The authors declare that they have no conflicts of interest with the contents of this article. The content is solely the responsibility of the authors and does not necessarily represent the official views of the National Institutes of Health.

This article contains Figs. S1–S5.

[1] Both authors contributed equally to this work.

[2] To whom correspondence should be addressed. Tel.: 973-972-8916; Fax: 973-972-8919; E-mail: sadoshju@njms.rutgers.edu.

[3] The abbreviations used are: CVD, cardiovascular disease; YAP, Yes-associated protein; CM, cardiomyocyte; MI, myocardial infarction; PO, pressure overload; TAC, transverse aortic constriction; GAPDH, glyceraldehyde-3-phosphate dehydrogenase; ANOVA, analysis of variance; DAPI, 4′,6-diamidino-2-phenylindole; TUNEL, terminal deoxynucleotidyltransferase-mediated dUTP nick end labeling; LVW, left ventricular weight; TL, tibia length; lung W, lung weight; PI3K, phosphatidylinositol 3-kinase; LV, left ventricular; ANF, atrial natriuretic factor; FS, fractional shortening.

© 2019 Byun et al. Published under exclusive license by The American Society for Biochemistry and Molecular Biology, Inc.

ation of microvasculature leads to an inability to maintain an efficient blood supply in response to CM enlargement. The resulting supply of nutrients is inadequate and promotes metabolic dysfunction and, eventually, heart failure.

PO stress increases ventricular strain. Interestingly, the Hippo pathway is regulated by mechanical stress (9). Previous work demonstrated that increased force causes up-regulation of YAP activity (10, 11). The small G-protein RhoA is a critical modulator of the actin cytoskeleton and plays a key role in both actin stress fiber formation and focal adhesion complex assembly in many cell types (12). In addition, RhoA has been shown to promote the activation of YAP in HEK293 cells through a mechanism dependent upon cytoskeletal integrity (13, 14). Prior studies have shown that RhoA affords cardioprotection *in vivo* and acts as a mediator of protein kinase D and Akt activation (15, 16). However, it remains unknown whether RhoA modulates Hippo-YAP in CMs or whether this potential mechanism influences the adaptive hypertrophic response to PO.

To elucidate the role of YAP in CMs during acute PO, we subjected control and CM-specific heterozygous YAP knockout mice (YAP-CHKO) to PO or sham operation. Our data demonstrate that, in response to PO, YAP is activated in the myocardium through a RhoA-dependent mechanism. Haploinsufficiency of YAP in CMs led to attenuated hypertrophy, but increased fibrosis and apoptosis, and decreased cardiac function during PO. These findings suggest that activation of endogenous YAP during PO mediates adaptive hypertrophy and protects the heart against PO-induced cardiac dysfunction.

Results

YAP is activated in response to PO

To examine whether YAP is activated in the heart in response to PO, wildtype (WT) mice were subjected to transverse aortic constriction (TAC) or sham operation and sacrificed at time points ranging from 6 h to 7 days. Under our experimental conditions, TAC significantly increased left ventricular (LV) weight/tibia length (LVW/TL), an index of cardiac hypertrophy, at 7 days in WT mice. Although TAC transiently increased lung weight/tibia length (lung W/TL), an index of lung congestion, 1 h after TAC, the index returned to baseline thereafter up to 7 days (Fig. S1). Immunoblot analyses of LV homogenates showed a significant increase in YAP protein 7 days after TAC compared with sham operation (Fig. 1*A*). YAP mRNA expression, as evaluated by quantitative PCR, was not significantly altered after TAC (Fig. 1*B*), suggesting that YAP protein up-regulation is due to increased translation or stabilization. Phosphorylation of YAP at Ser-127 promotes its cytosolic retention and subsequent degradation (17). The ratio of Ser-127–phosphorylated YAP to total YAP was decreased after TAC in a time-dependent manner compared with sham (Fig. 1*C*). Decreased YAP phosphorylation can favor YAP retention in the nucleus. Phosphorylation of YAP at Ser-397 promotes its proteolytic degradation (18). The ratio of Ser-397 phosphorylated YAP to total YAP also decreased 7 days after TAC (Fig. 1*D*), suggesting that YAP is stabilized. Although the level of Lats2, the kinase responsible for YAP phosphorylation at Ser-127, was increased in a time-dependent manner after TAC, phosphorylated Lats2/total Lats2 did not change significantly (Fig. 1*E*). This suggests that YAP regulation during acute PO may be independent of Lats2.

Nuclear localization of YAP, as evaluated by immunofluorescence, was increased 7 days after TAC compared with sham operation (Fig. 1*F*). In addition, subcellular fractionation was conducted to separate cytosolic and nucleus-enriched fractions. The level of YAP in both cytosolic and nuclear fractions was increased significantly after TAC, compared with sham (Fig. 1, *G* and *H*).

To test whether TAC-induced up-regulation and nuclear accumulation of YAP take place in CMs, CMs were isolated from mouse hearts subjected to 1 week of TAC or sham operation. Immunofluorescent staining showed that the number of CMs with nuclear YAP staining was significantly greater in hearts subjected to 1 week of TAC than in those subjected to sham operation (Fig. S2, *A* and *B*). Immunoblot analyses of CM lysates showed that phospho-YAP/total YAP was significantly smaller and total YAP was greater in myocytes isolated from mouse hearts subjected to TAC than in those isolated from sham-operated hearts. Taken together, these results indicate that total YAP protein and its nuclear localization in CMs are increased 1 week after TAC (Fig. S2, *C*, *D*, and *E*). In a recent study (19), we found that YAP is inactivated during the decompensated phase of cardiac hypertrophy. Thus, we sought to determine the functional significance of cardiac YAP activation during the compensated phase of PO.

TAC-induced activation of YAP was attenuated in heterozygous cardiac-specific YAP knockout (KO) mice

To investigate the functional significance of YAP activation during the compensated phase of PO, we used heterozygous CM-specific YAP KO mice ($Yap^{+/flox}$;$Cre^{\alpha MHC}$, referred to as YAP-CHKO) (5). We used heterozygous KO mice because homozygous CM-specific YAP KO mice rapidly develop heart failure at baseline, even when a tamoxifen-inducible system is used. We subjected WT mice ($Yap^{+/flox}$) and YAP-CHKO mice to either TAC for 7 days or sham operation. The level of YAP in the heart was significantly lower in YAP-CHKO mice than in WT mice subjected to either sham operation or TAC (Fig. 2, *A* and *B*). *Ctgf* (connective tissue growth factor), an established YAP target gene (20), was increased in WT mouse hearts 7 days after TAC, and this up-regulation was attenuated in YAP-CHKO mouse hearts (Fig. 2*C*). Similar results were obtained for *Ankrd1* (ankyrin repeat domain-containing protein), another YAP target gene (Fig. 2*D*) (21). These results suggest that YAP-CHKO mice are a useful model for evaluating the function of endogenous YAP in the heart after TAC.

Down-regulation of YAP attenuated PO-induced cardiac hypertrophy

We asked whether down-regulation of endogenous YAP affects the initial TAC-induced hypertrophic response. At 7 days after TAC, postmortem measurements revealed that LVW/TL was significantly increased in both WT and YAP-CHKO TAC groups compared with sham. However, we observed a significant attenuation of LVW/TL in YAP-CHKO

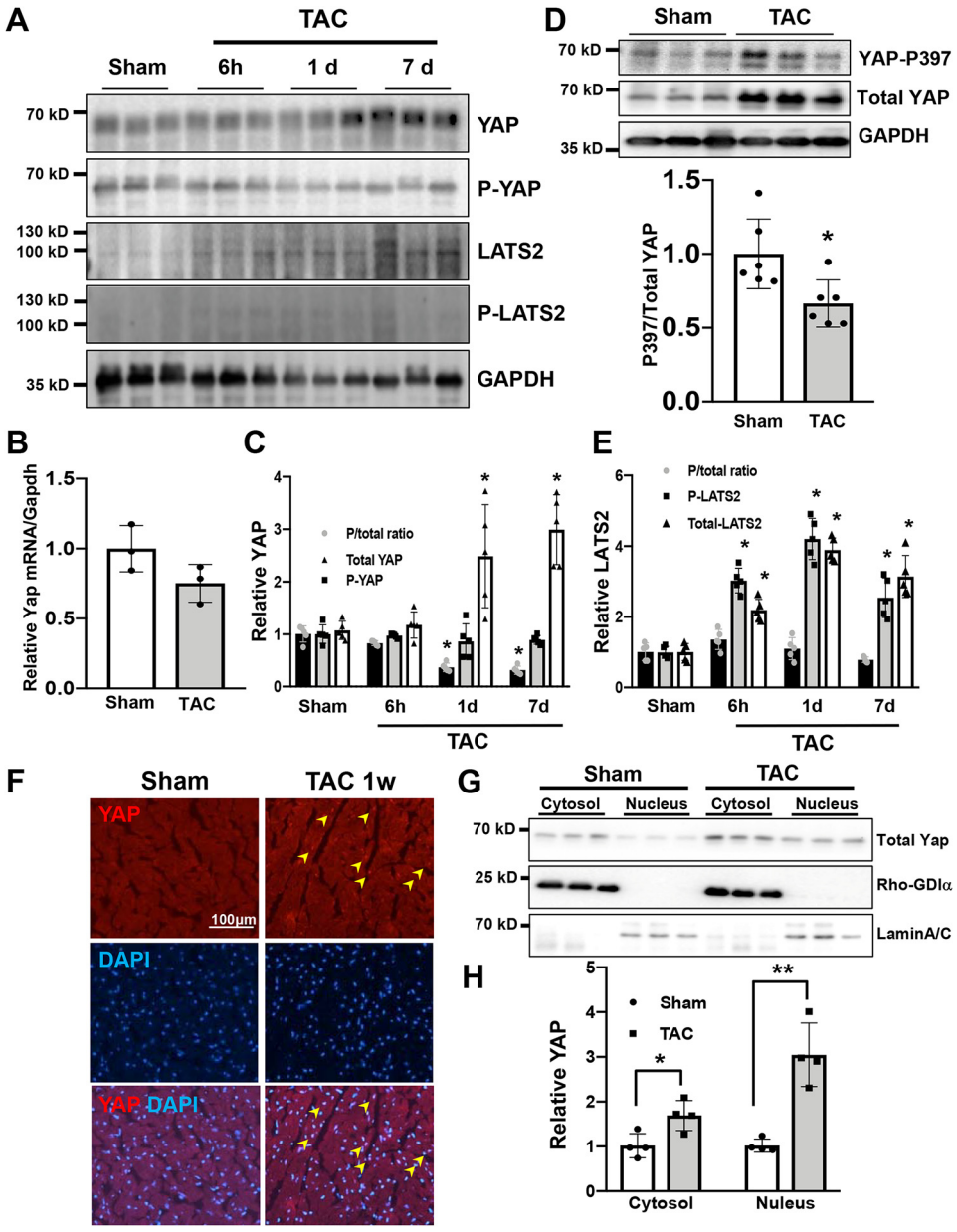

Figure 1. YAP is activated after acute PO. Wildtype (WT) mice were subjected to TAC. The hearts were harvested at indicated time points (6 h to 7 days (*d*)). *A*, immunoblot analyses were performed to determine the phosphorylation status of YAP and Last2 in ventricular lysates. $n = 5$. *B*, mRNA expression of YAP in the mouse heart was measured by quantitative real-time PCR assays. $n = 3$. *C*, quantification of Ser-127–phosphorylated YAP and total YAP. *D*, immunoblot analyses of Ser-397–phosphorylated YAP and total YAP. *E*, quantification of phosphorylated Lats2 and total Lats2. *F*, immunostaining for YAP 7 days after TAC in the WT mouse heart. DAPI was used for nuclear staining. $n = 4$. *G*, subcellular localization of endogenous YAP in mouse ventricular extracts 7 days after TAC. Rho-GDIα and lamin A/C served as markers of cytosol- and nucleus-enriched fractions, respectively. $n = 4$. *H*, quantification of the data shown in *G*. The data are expressed as ratios relative to the mean value of the sham group. Data in *graphs* represent mean ± S.D.; *, $p < 0.05$; **, $p < 0.01$, compared with Sham. Statistical analyses were conducted with ANOVA or Student's *t* test. Post hoc analysis was conducted with Tukey's test.

versus WT in response to TAC (Fig. 3*A*). Lung W/TL was significantly increased in both WT and YAP-CHKO TAC groups compared with sham, and there was no significant difference in lung W/TL between YAP-CHKO *versus* WT in response to TAC (Fig. 3*B*). To determine whether the blunted hypertrophy was accompanied by a reduction in individual CM size, we performed a histological analysis. Measurement of CM cross-sectional area revealed a significant attenuation in YAP-CHKO hearts compared with WT mice 7 days after TAC (Fig. 3*C*). mRNA expression of atrial natriuretic factor (ANF) was increased significantly after TAC in both WT and YAP-CHKO mice compared with respective sham-operated mice (Fig. 3*D*). Interestingly, however, YAP-CHKO mice exhibited a greater increase in ANF mRNA after TAC than WT mice, consistent with the observation that YAP-CHKO mice exhibit greater LV wall stress than WT mice (see below). Down-regulation of YAP also inhibited increases in CM cell size induced by isoproterenol, a β-adrenergic receptor agonist, suggesting that endogenous YAP is essential in mediating hypertrophy in CMs (Fig. S3).

To evaluate how down-regulation of YAP affects cardiac function during acute PO, echocardiography was performed 7

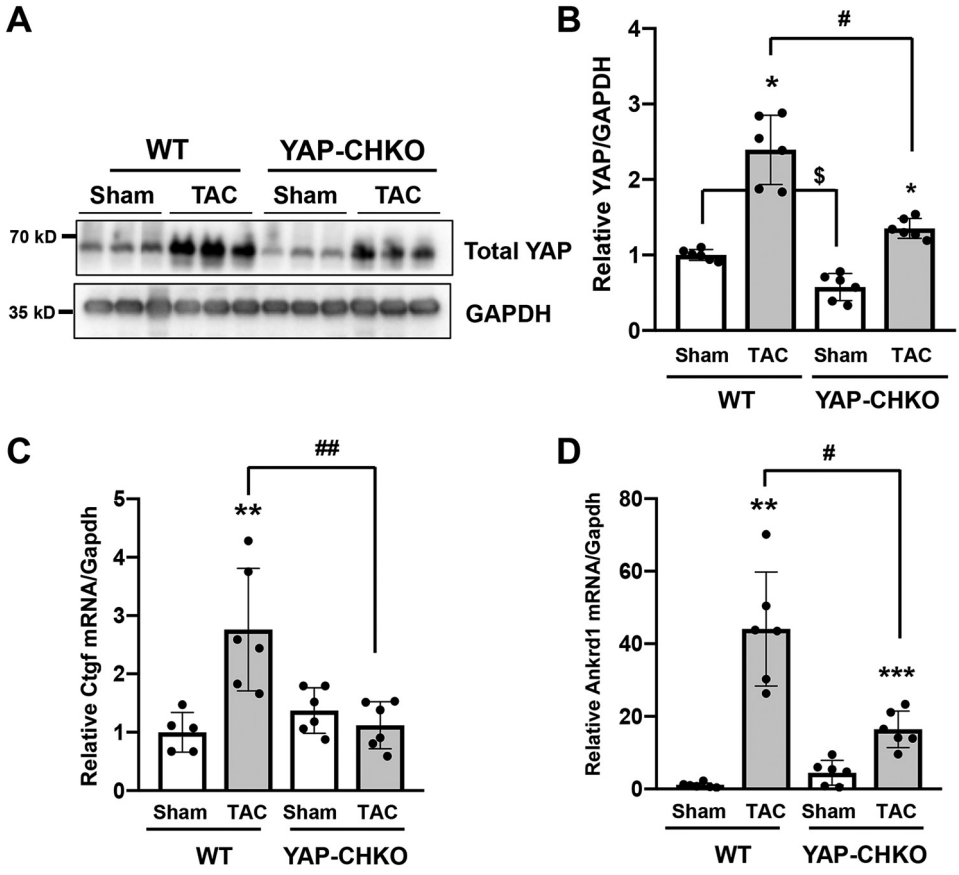

Figure 2. PO-induced up-regulation of YAP was inhibited in YAP-CHKO mice. TAC or sham operation was applied to WT or YAP-CHKO mice for 7 days. *A* and *B*, whole-heart lysates were subjected to immunoblotting with anti-YAP antibody. GAPDH antibody was used as loading control. Data are expressed as a ratio compared with the mean value of the WT-sham group. $n = 6$ per group. *C* and *D*, total RNA was extracted from the heart and subjected to quantitative RT-PCR analyses. Relative mRNA expression of Ctgf (*C*) and Ankrd (*D*) is shown. $n = 5–6$. The data are expressed as ratios relative to the mean value of the WT-sham group. Data in *graphs* represent mean ± S.D.; **, $p < 0.01$; ***, $p < 0.005$ compared with Shams; $, $p < 0.05$ in comparison with WT-sham and YAP-CHKO-Sham; #, $p < 0.05$; ##, $p < 0.01$, in comparison with WT-TAC and YAP-CHKO-TAC. Statistical analyses were conducted with ANOVA. Post hoc analysis was conducted with Tukey's test.

days after TAC (Table 1). YAP-CHKO and WT mice exhibited similar baseline LV systolic function. In response to 7 days of TAC, WT mice exhibited preserved systolic function, whereas YAP-CHKO mice exhibited significantly decreased LV function, as evaluated by fractional shortening (%FS) (Fig. 4, *A* and *B*). LV end-diastolic diameter after TAC was significantly greater in YAP-CHKO than in WT mice (Fig. 4*C*), whereas wall thickness was similar between YAP-CHKO and WT mice (Table 1). Laplace's Law states that the wall stress (WS) of the ventricle is proportional to the ventricular pressure (P) and its diameter (R) and is inversely proportional to the ventricular wall thickness (T), given by the formula $WS = P{\cdot}R/2T$. Echocardiographic and hemodynamic measurements indicated that LV wall stress was significantly elevated in YAP-CHKO hearts compared with WT hearts 7 days after TAC (Fig. 4*D*).

Invasive hemodynamic analyses indicated that LV end-diastolic pressure (LVEDP) was significantly elevated in WT mice 7 days after TAC and was further elevated in YAP-CHKO mice (Fig. 4*E* and Table 2). These data suggest that YAP in CMs is required for the maintenance of cardiac function and that decreased levels of YAP result in rapid chamber dilation and transition to heart failure during acute PO.

YAP down-regulation augmented apoptosis and fibrosis in response to PO

Myocardial apoptosis and fibrosis were evaluated by TUNEL and Masson's Trichrome staining, respectively (Fig. 5). PO for 7 days was not sufficient to induce a significant increase in either myocardial apoptosis or fibrosis in WT mice. However, we observed significant increases in both apoptosis and fibrosis in YAP-CHKO hearts following 7 days of TAC compared with WT mouse hearts (Fig. 5). These results suggest that endogenous YAP in CMs protects the heart against apoptosis and fibrosis during the acute phase of PO.

Heterozygous down-regulation of YAP inhibited cell cycle re-entry in response to PO in CMs

YAP promotes cell cycle progression and/or cell proliferation in noncardiac cell types, as well as in CMs in the embryonic heart (22, 23). Although the adult heart has a limited capacity for regeneration, a small population of CMs can re-enter the cell cycle in response to injury and may confer a regenerative benefit to the heart (24). Therefore, we investigated the effect of YAP deletion on CM proliferation under acute PO stress. We stained heart sections for Ki-67 and the CM marker troponin-T. Quantitative analyses revealed that

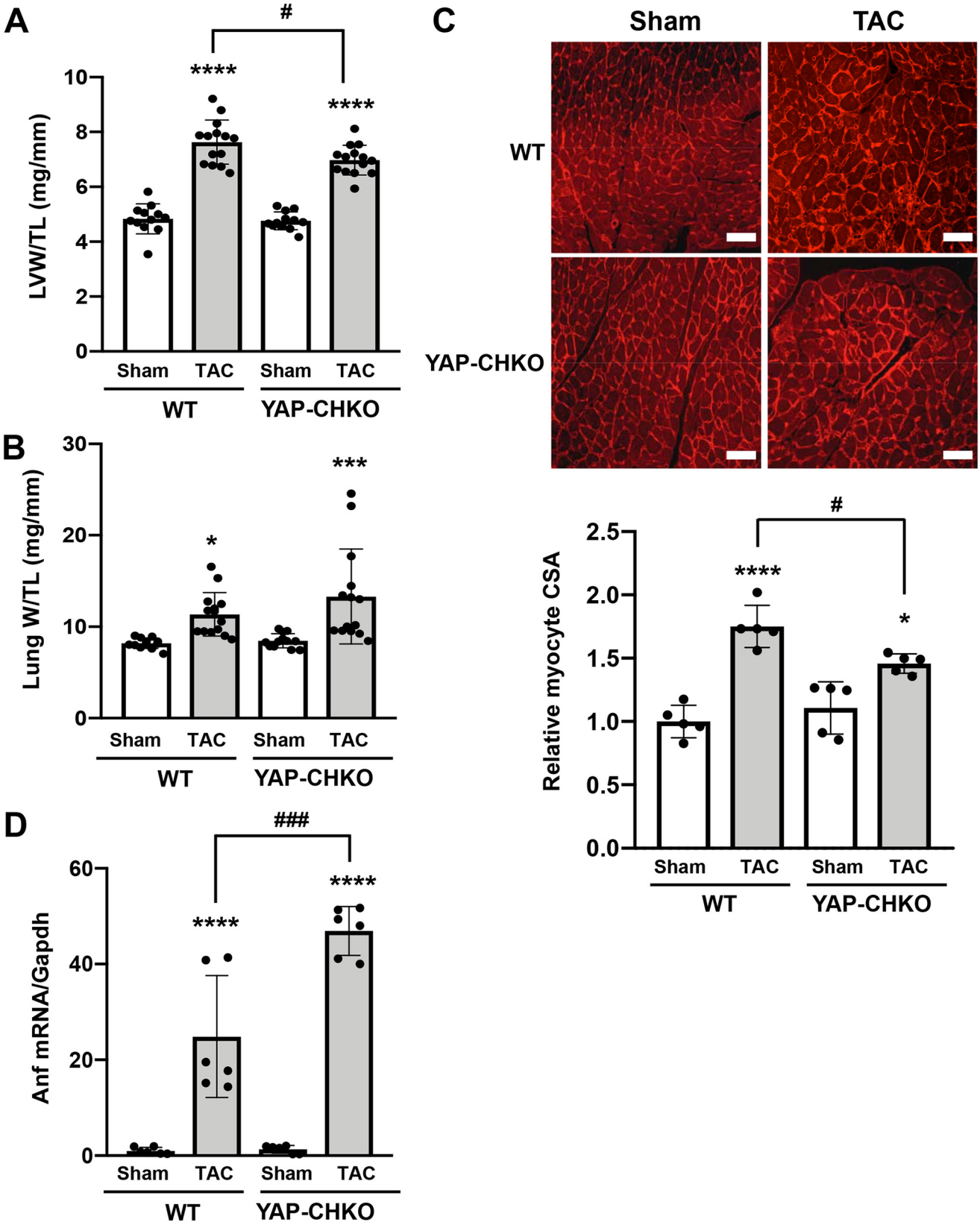

Figure 3. Heterozygous down-regulation of YAP significantly attenuates PO-induced cardiac hypertrophy. TAC was applied to WT or YAP-CHKO mice for 1 week. *A*, LVW/TL. $n = 12–14$. *B*, lung W/TL. $n = 12–14$. *C*, cardiomyocyte cross-sectional area (*CSA*) was evaluated with wheat germ agglutinin staining. Values are relative to the WT-sham group. Representative images from each group are shown in the *upper panel*. *Scale bars*, 200 μm. $n = 5$ per group. *D*, mRNA expression of Anf was evaluated with quantitative RT-PCR. $n = 6$. Values are mean ± S.D. relative to the WT-sham group. *, $p < 0.05$; ***, $p < 0.001$; ****, $p < 0.0001$; *versus* shams. #, $p < 0.05$; ###, $p < 0.001$ in comparison with WT-TAC and YAP-CHKO-TAC. Statistical analyses were conducted with ANOVA. Post hoc analysis was conducted with Tukey's test.

Table 1

Echocardiographic analyses of WT and YAP-CHKO mice 7 days after TAC

Data are presented as mean ± S.D. The following abbreviations are used: DSEP WT, diastolic septal wall thickness; LVEDD, left ventricular end diastolic dimension; DPWT, diastolic posterior wall thickness; LVESD left ventricular end systolic dimension; LVEF, left ventricular ejection fraction; %FS, fractional shortening.

	WT		YAP-CHKO	
	Sham	TAC	Sham	TAC
n	12	14	12	14
DSEP WT (mm)	0.79 ± 0.05	0.81 ± 0.10	0.77 ± 0.09	0.83 ± 0.09
LVEDD (mm)	3.44 ± 0.30	3.35 ± 0.24	3.58 ± 0.28	3.89 ± 0.29[a]
DPWT (mm)	0.67 ± 0.07	0.72 ± 0.11	0.73 ± 0.06	0.73 ± 0.12
LVESD (mm)	2.30 ± 0.35	2.26 ± 0.35	2.57 ± 0.44	3.18 ± 0.37
EF (%)	68.4 ± 13.1	66.5 ± 15.4	62.1 ± 12.1	44.2 ± 14.0[a,b]
%FS (%)	33.12 ± 9.53	32.18 ± 11.23	28.45 ± 7.97	18.27 ± 7.18[a,b]

[a] $p < 0.05$ *versus* WT-TAC is shown.
[b] $p < 0.05$ *versus* YAP-CHKO-SHAM is shown. Statistical analyses were conducted with ANOVA. Post hoc analysis was conducted with Tukey's test.

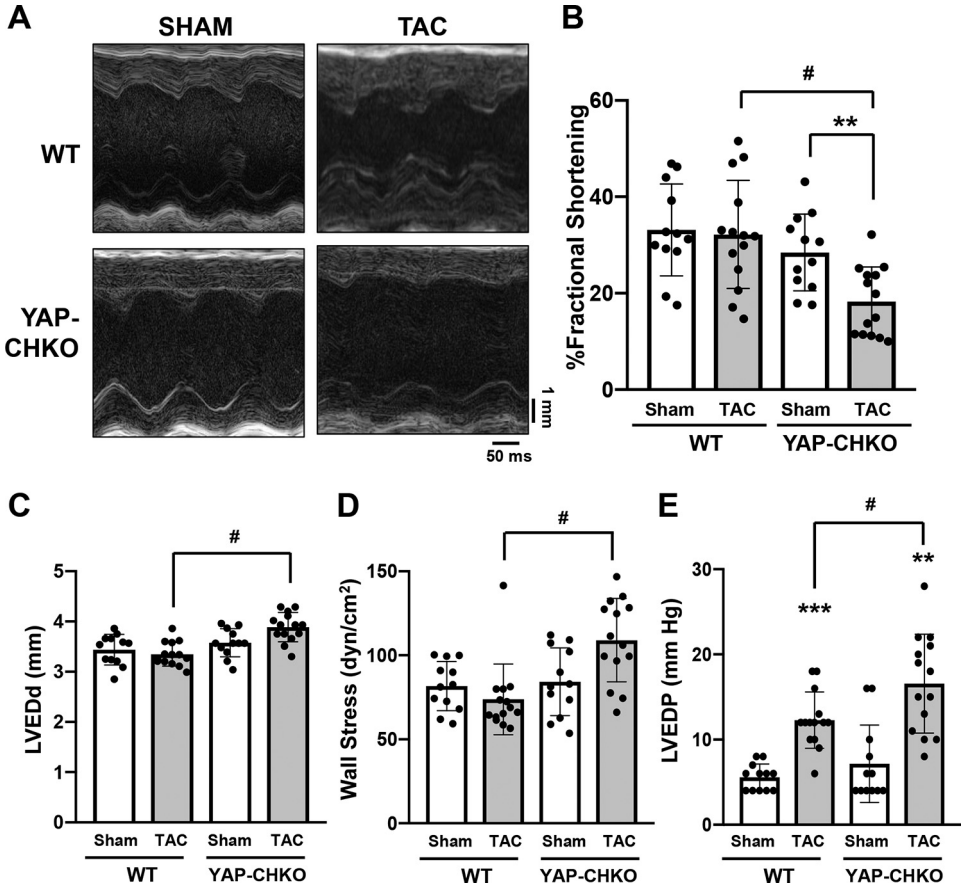

Figure 4. TAC-induced cardiac dysfunction was exacerbated in YAP-CHKO mice. WT and YAP-CHKO mice were subjected to either TAC or sham operation for 7 days. Echocardiography and hemodynamic analyses were performed before euthanasia 7 days after TAC or sham operation. *A*, representative images of M mode echocardiography. *B*, % fractional shortening. *C*, left ventricular end-diastolic diameter (*LVEDd, mm*). *D*, wall stress calculated using the data set obtained by echocardiography and hemodynamic measurement. *E*, left ventricular end-diastolic pressure (*LVEDP, mm Hg*) evaluated with a Millar catheter. n = 12–14 per group. *B–E*, values are mean ± S.D. **, $p < 0.01$; ***, $p < 0.001$ *versus* shams; #, $p < 0.05$ in comparison with WT-TAC and YAP-CHKO-TAC. Values are means ± S.D. Statistical analyses were conducted with ANOVA. Post hoc analysis was conducted with Tukey's test.

there was a small population of Ki-67–positive CMs in WT hearts in response to PO (Fig. 6, *A* and *B*). However, we observed no significant increase in the number of Ki-67–positive CMs in YAP-CHKO mouse hearts after TAC compared with sham. These data suggest that YAP deficiency in CMs results in repressed CM cell cycle re-entry in response to short-term PO.

Stretch-induced YAP activation in CMs is mediated by RhoA

Although the level of Ser-127–phosphorylated YAP/total YAP was decreased 7 days after TAC, the level of phosphorylated Lats2/total Lats2, the predominant YAP kinase, did not change significantly. The small GTPase RhoA is associated with CM hypertrophy and the protective signaling mechanism within the myocardium *in vivo* (12, 15, 25). To elucidate the underlying mechanism of YAP activation in response to PO, we investigated the involvement of RhoA signaling and mechanical stress. To this end, we applied cyclic stretch to CMs to induce hypertrophy (26). CMs were subjected to 1 h of cyclic stretch, and subcellular fractions were prepared from cell lysates. We found that YAP was increased in the nuclear fraction after stretch compared with the control unstretched CMs. Pretreat-

Table 2

Hemodynamic measurements of WT and YAP-CHKO mice 7 days after TAC

Data are presented as mean ± S.D. The following abbreviations are used: LVEDP, left ventricular end diastolic pressure; +d*P*/d*t* and −d*P*/d*t*, change in pressure over time; PG, pressure gradient.

	WT		YAP-CHKO	
	Sham	TAC	Sham	TAC
n	10	14	10	14
+d*P*/d*t* (mm Hg/s)	7750 ± 1327	5839 ± 1403[a]	5625 ± 1579[b]	4964 ± 1397[c]
−d*P*/d*t* (mm Hg/s)	7520 ± 1079	6339 ± 1950	5125 ± 1165[b]	4732 ± 1908[d]
LVEDP (mm Hg)	5.58 ± 1.56	12.29 ± 3.29[a]	7.8 ± 4.5	16.57 ± 5.80[d,e]
PG (mm Hg)	NA	72.86 ± 24.1	NA	53.14 ± 22.1

[a] $p < 0.05$ *versus* WT-Sham mice.
[b] $p < 0.01$ *versus* WT-Sham mice.
[c] $p < 0.001$ *versus* WT-TAC mice.
[d] $p < 0.001$ *versus* WT-TAC mice.
[e] $p < 0.05$ *versus* YAP-CHKO-Sham. Statistical analyses were conducted with ANOVA. Post hoc analysis was conducted with Tukey's test.

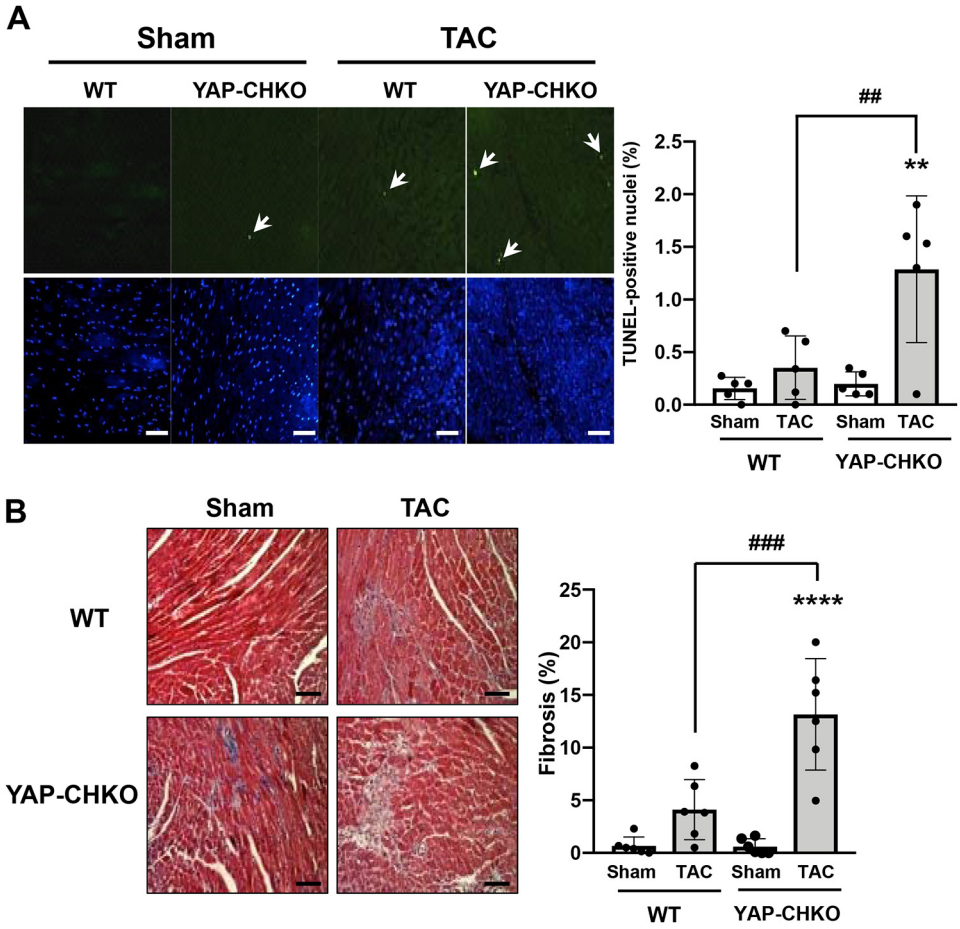

Figure 5. TAC-induced apoptosis and fibrosis were significantly increased in YAP-CHKO mice. WT and YAP-CHKO mice were subjected to either TAC or sham operation for 7 days. *A, left,* representative images of TUNEL staining and DAPI staining from each group. TUNEL-positive CMs are indicated by *white arrows*. *Scale bars*, 100 μm. *A, right,* number of TUNEL-positive CMs/the total number of nuclei. Values are mean ± S.D. $n = 5$. *B, left*, Masson's trichrome staining showing interstitial fibrosis. Representative images from each group are shown. *Scale bars*, 100 μm (*right*). The quantitative analysis of the fibrotic areas. $n = 6$. Values are the means ± S.D. ***, $p < 0.0005$; ****, $p < 0.0001$ *versus* shams. ##, $p < 0.01$; ###, $p < 0.0005$ in comparison with WT-TAC and YAP-CHKO-TAC. Statistical analyses were conducted with ANOVA. Post hoc analysis was conducted with Tukey's test.

ment of CMs with C3 exoenzyme, a selective inhibitor of RhoA activation, abolished the nuclear accumulation of YAP (Fig. 7*A*). Importantly, RhoA was activated 1 day and 7 days after TAC, time points at which YAP was up-regulated (Fig. 7*B*). To determine whether RhoA activation is sufficient to promote YAP nuclear localization, CMs were transduced with adenovirus harboring either constitutively active RhoA (RhoA (Q63L)) or GFP. YAP protein was more abundant in the nucleus of CMs with constitutively active RhoA than in CMs with GFP (Fig. 7, *C* and *D*). We also found that sphingosine 1-phosphate, a potent activator of RhoA in CMs, increased nuclear YAP, an effect that was blocked by concomitant C3 treatment (Fig. S4). These data suggest that RhoA activation is sufficient to induce YAP activation and is necessary for stretch- and agonist-induced YAP nuclear localization in CMs.

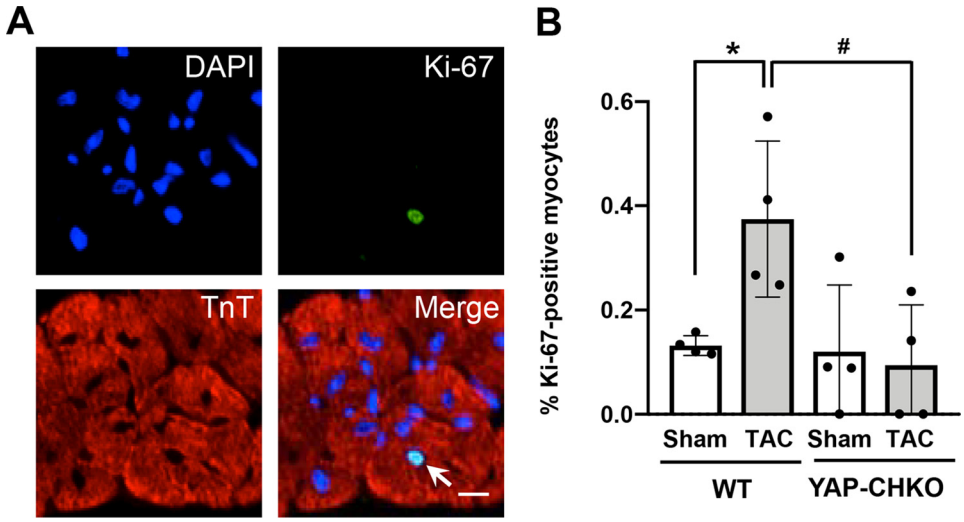

Figure 6. Heterozygous down-regulation of YAP inhibits CM cell cycle re-entry 7 days after TAC. WT and YAP-CHKO mice were subjected to either TAC or sham operation for 7 days. *A,* heart sections were stained with anti-Ki-67 (*green*), anti-troponin T (*red*), and DAPI (*blue*). The *arrow* indicates a Ki-67–positive CM. *B,* quantification of Ki-67–positive CMs (%) detected in WT and YAP-CHKO mouse hearts. $n = 4$. Values are mean ± S.D. *, $p < 0.05$ *versus* WT-sham; #, $p < 0.05$, comparison with WT-TAC and YAP-CHKO-TAC. Statistical analyses were conducted with ANOVA. Post hoc analysis was conducted with Tukey's test.

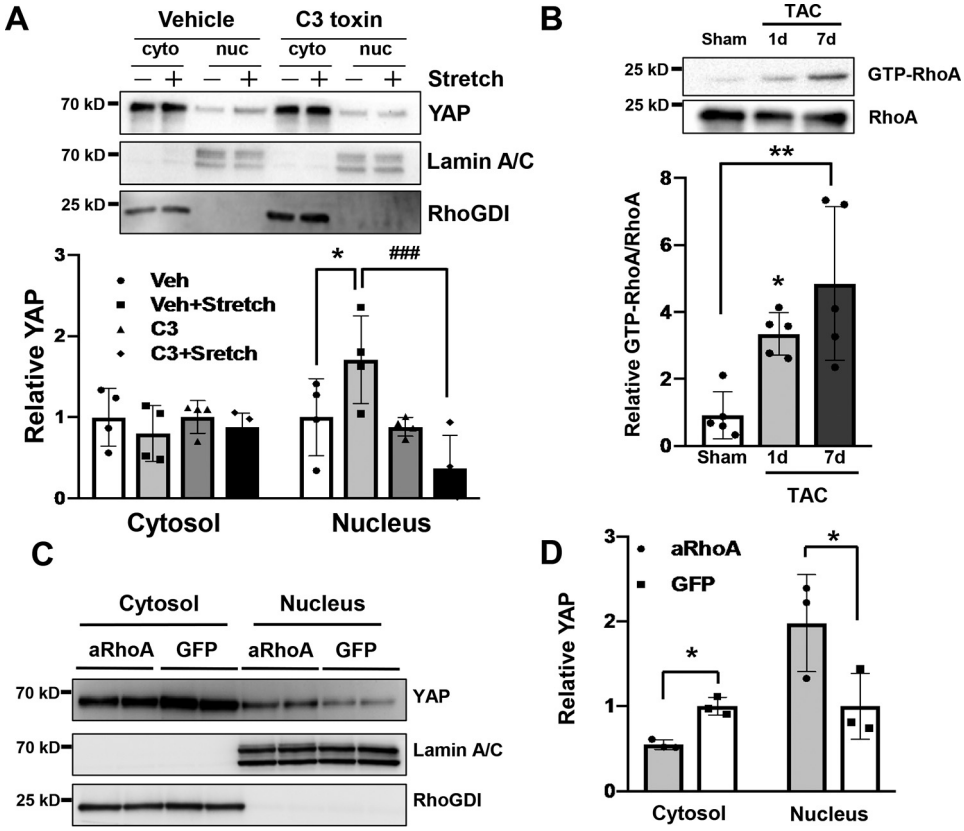

Figure 7. RhoA mediates activation of YAP in response to mechanical stress. *A*, cultured neonatal rat CMs were pre-incubated with either C3 toxin (1 mg/ml), an inhibitor of RhoA, or vehicle (*veh*) for 4 h before stretch stress. CMs were then cyclically stretched by 20% for 1 h. Cytosolic (*cyto*)- and nucleus (*nuc*)-enriched fractions were prepared by subcellular fractionation. Representative immunoblots are shown in *A*. Rho-GDI and lamin A/C served as markers of cytosolic- and nucleus-enriched fractions, respectively. The experiments were repeated four times. *, $p < 0.05$ in comparison with vehicle (*Veh*) and vehicle + stretch; #, $p < 0.05$ in comparison with vehicle + stretch and C3 + stretch. *B*, mice were subjected to either sham or TAC for 1 or 7 days, and then heart homogenates were prepared. The RhoA-binding domain of rhotekin was used to selectively pull down activated GTP-bound RhoA. Samples were analyzed by SDS-PAGE. The relative binding of GTP-loaded RhoA to rhotekin is shown. $n = 6$. *, $p < 0.05$, *versus* sham. *C* and *D*, neonatal rat CMs were transduced with either GFP or active RhoA (RhoA (Q63L), aRhoA) adenovirus. *C*, cytosolic- and nucleus-enriched fractions were prepared by subcellular fractionations and then subjected to immunoblot analyses with anti-YAP antibody. Immunoblots with anti-RhoGDI and anti-lamin A/C antibodies were conducted to assess the purity of each fraction. *D*, quantification of the data shown in *C*. $n = 4$. Data are mean ± S.D. *, $p < 0.05$; **, $p < 0.01$, comparison with aRhoA and GFP. Statistical analyses were conducted with ANOVA. Post hoc was conducted with Tukey's test.

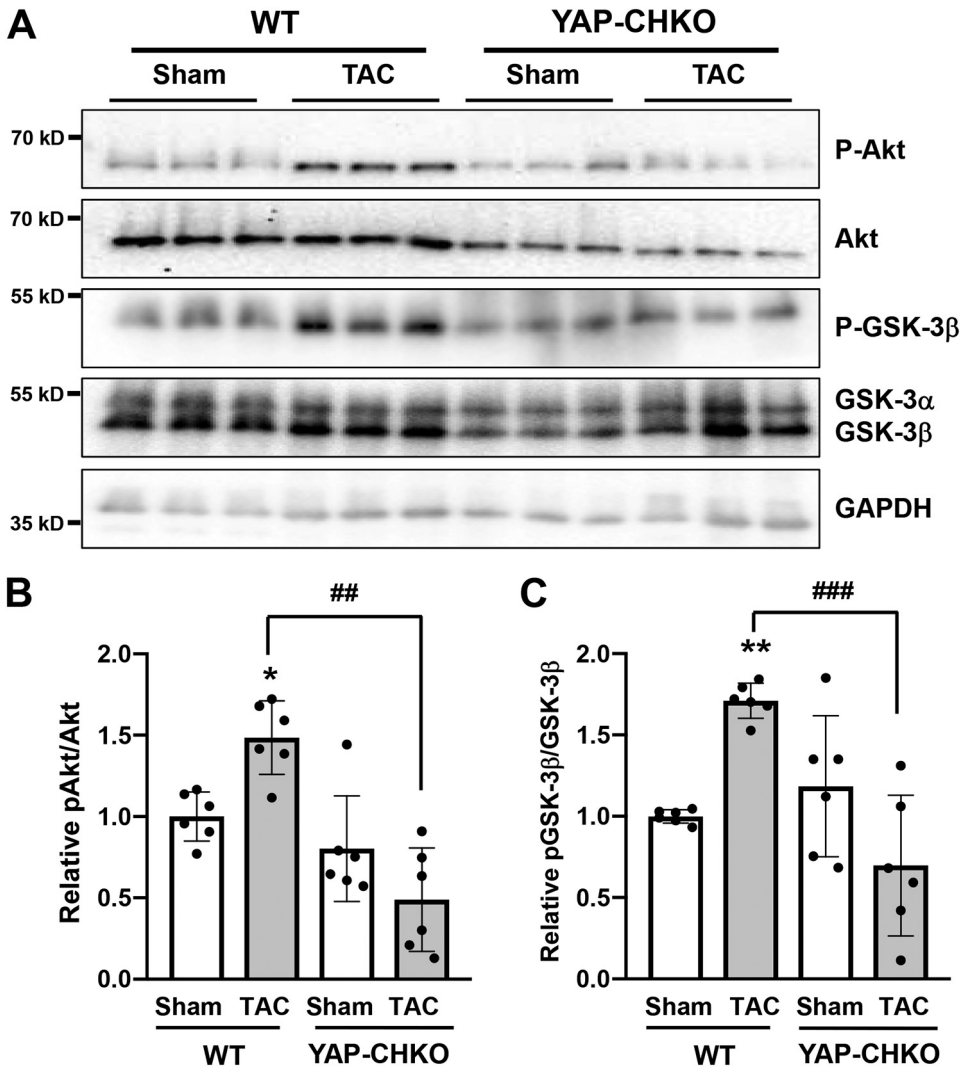

Figure 8. Heterozygous down-regulation of YAP inhibits Akt phosphorylation after 1 week of TAC. WT and YAP-CHKO mice were subjected to either TAC or sham operation for 7 days. *A*, whole-heart lysates were subjected to immunoblotting for Thr-308 –phosphorylated and total Akt or Ser-9 –phosphorylated and total GSK-3β antibody. GAPDH antibody was used as loading control. Representative immunoblots are shown. *B*, quantification of relative pAkt/Akt shown in *A*. *C*, quantification of relative pGSK-3β/GSK-3β shown in *A*. *B* and *C*, data are normalized by the mean value in the WT-sham group. Values are mean ± S.D. $n = 6$ animals per group. *, $p < 0.05$; **, $p < 0.01$ *versus* sham; ##, $p < 0.01$; ###, $p < 0.0005$, compared with WT-TAC and YAP-CHKO-TAC. Statistical analyses were conducted with ANOVA. Post hoc analysis was conducted with Tukey's test.

YAP-CHKO mice showed a dampened Akt response during PO

We next investigated the molecular mechanism through which YAP mediates cardiac hypertrophy during the acute phase of PO. Akt signaling has been shown to modulate cardiac hypertrophy, and our previous work demonstrated a link between YAP and Akt in CMs (27–29). We therefore examined whether Akt activation was altered in YAP-CHKO hearts following PO stress. First, we confirmed that Akt phosphorylation at Ser-473 was increased at 7 days post-TAC in WT mouse hearts (Fig. 8, *A* and *B*). Interestingly, we observed that the increase in p-Akt was significantly diminished in YAP-CHKO hearts compared with WT hearts after TAC; however, we saw no difference in Akt phosphorylation in YAP-CHKO hearts at baseline (Fig. 8, *A* and *B*). We observed a similar trend in phosphorylation of GSK-3β, an established substrate of active Akt (Fig. 8, *A* and *C*). These data indicate impaired Akt activation in response to acute PO in hearts deficient for YAP and suggest that YAP mediates Akt signaling in this setting.

YAP is a negative regulator of PTEN

Second, we sought to determine how YAP regulates Akt in this context. The PI3K/Akt pathway is negatively regulated by the lipid phosphatase, PTEN. PTEN dephosphorylates phosphatidylinositol 3,4,5-trisphosphate to phosphatidylinositol 4,5-bisphosphate, thereby antagonizing the PI3K signaling cascade (30). Recently, it was reported that PTEN is a critical mediator of YAP function (31). To investigate a potential link between YAP and PTEN in the heart, we first evaluated PTEN expression. Hearts were harvested from 8-week-old control ($Yap^{flox/flox}$), heterozygous ($YAP^{+/flox};Cre^{\alpha MHC}$), and homozygous ($YAP^{flox/flox};Cre^{\alpha MHC}$) YAP KO mice. We observed that down-regulation of YAP dose-dependently increased PTEN expression in the mouse heart (Fig. 9*A*). As a complementary approach, we transduced neonatal rat CMs with YAP adenovirus or LacZ control. We found that PTEN expression was significantly decreased in response to YAP overexpression (Fig. 9*B*). These results suggest that YAP

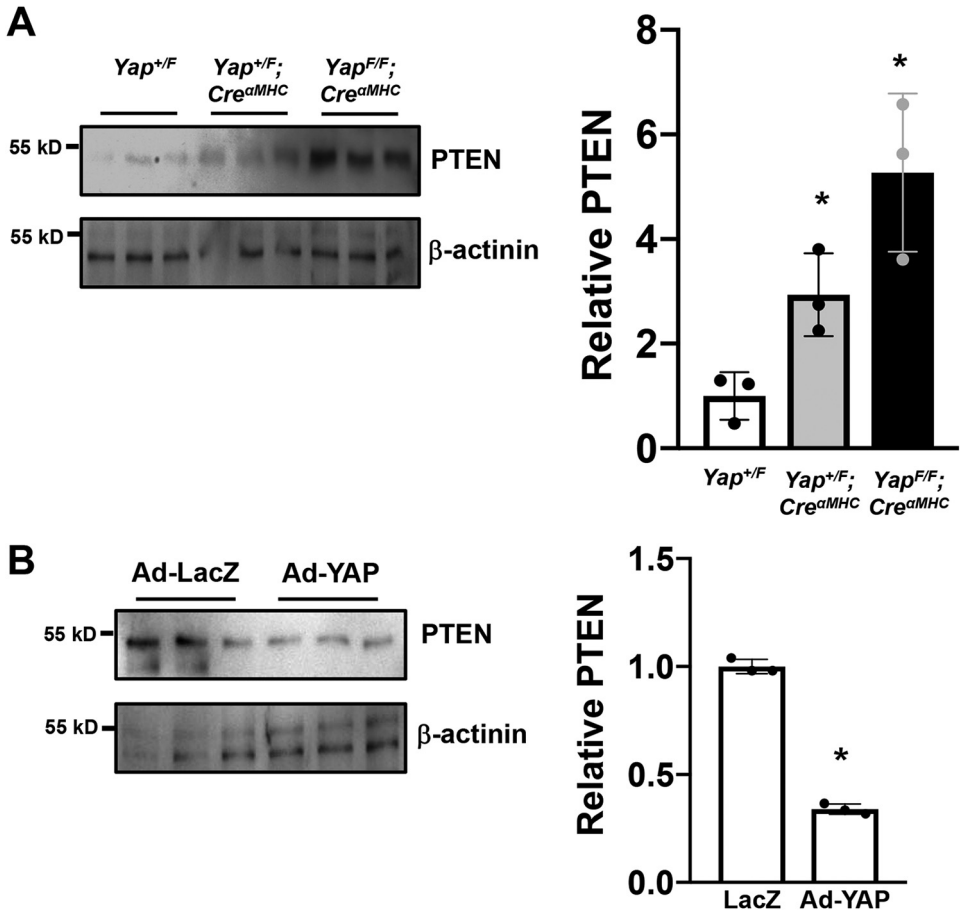

Figure 9. YAP negatively regulates PTEN in CMs. *A*, hearts were harvested from $Yap^{+/F}$, $Yap^{+/F}$;$Cre^{\alpha MHC}$, and $Yap^{F/F}$;$Cre^{\alpha MHC}$ mice under baseline conditions. Whole-heart lysates were subjected to immunoblotting for PTEN and β-actinin. The data are normalized by the mean value in $Yap^{+/F}$ group. In the presence of decreased of YAP expression, PTEN expression was increased. Values are the means ± S.D. *, $p < 0.05$ *versus* $Yap^{+/F}$. $n = 3$. *B*, neonatal rat CMs were transduced with LacZ control (*Ad-LacZ*) or YAP adenovirus (*Ad-YAP*). Cell lysates were subjected to immunoblotting for PTEN and β-actinin. The data are normalized by the mean value of the LacZ-transduced CMs. The experiments were repeated four times. Values are mean ± S.D. *, $p < 0.05$ *versus* the LacZ-transduced CMs. Statistical analyses were conducted with ANOVA or Student's *t* test. Post hoc analysis was conducted with Tukey's test.

stimulates Akt activation through down-regulation of PTEN in CMs.

Discussion

Our results show that endogenous YAP is activated in the heart during the acute phase of PO. Haploinsufficiency of YAP suppresses cardiac hypertrophy in response to PO and worsens cardiac dilation and dysfunction. Thus, activation of endogenous YAP plays an essential role in mediating cardiac hypertrophy and survival of CMs during the acute phase of PO. Although previous studies suggested that YAP primarily controls proliferation of CMs or CM progenitors (22, 32), our results suggest that endogenous YAP also mediates cardiac hypertrophy in a context-dependent manner.

Does YAP mediate CM proliferation or hypertrophy?

The Hippo pathway negatively affects organ size by promoting apoptosis and inhibiting proliferation (33). Because growth of the adult heart in mammals occurs primarily through hypertrophy of CMs (34), whether or not the Hippo pathway also controls cardiac hypertrophy, namely cell enlargement without proliferation, is an intriguing question. Our previous work demonstrated that transgenic mice with cardiac-specific overexpression of Mst1 develop dilated cardiomyopathy with increased CM apoptosis. CM size in these mice was smaller than in nontransgenic controls despite dilation of the heart and increased wall stress (35). Lats2, a negative regulator of YAP, also inhibits hypertrophy of CMs during PO (36). Although these studies show that the major upstream components of the Hippo pathway negatively affect cardiac hypertrophy when they are overexpressed, whether or not endogenous Mst1 or Lats2 is involved in the regulation of cardiac hypertrophy during cardiac stress remains to be elucidated.

Experimentally, YAP gain-of-function that is induced by either overexpression of constitutively active YAP or by loss of Hippo pathway function (down-regulation of WW45) promotes myocardial regeneration by stimulating proliferation of either CMs or CM progenitors without evidence of CM hypertrophy (23, 32, 37). Overexpression of YAP in mouse embryonic hearts increases heart size by promoting CM proliferation without significantly changing CM size (22). These results lend support to the hypothesis that YAP does not promote CM hypertrophy. However, it should be noted that gain-of-function experiments may not necessarily reflect the function of endogenous YAP.

Using a loss-of-function mouse model, we show here that endogenous YAP plays an essential role in mediating cardiac hypertrophy during the early phase. Based on our current findings, together with our previous study demonstrating that endogenous YAP mediates cardiac hypertrophy after MI (5), we propose that endogenous YAP can control cardiac hypertrophy in a manner that is context-dependent. We have shown previously that YAP is activated in a small population of CMs located in the border zone of MI where CM cell cycle re-entry is stimulated (5). However, YAP is phosphorylated and inactivated in the majority of CMs located in the remote area even in that context (5). Interestingly, down-regulation of YAP in the whole heart prevents overall cardiac hypertrophy, and the mean diameter of individual CMs in YAP-CHKO mice was smaller than in control mice in the presence of either volume overload (4) or PO (this study). We speculate that although activation of YAP can stimulate CM cell cycle re-entry or proliferation under some conditions, such as in the post-MI border zone, at baseline or when modestly activated YAP also controls cardiac hypertrophy.

As reported previously (24, 39), we confirm here that a modest population of CMs shows signs of cell cycle re-entry during the acute phase of PO. Because the number of Ki-67–positive CMs was significantly decreased in YAP-CHKO mice, endogenous YAP may play an important role in CM cell cycle re-entry or proliferation. However, because we observed both smaller CMs and less CM cell cycle re-entry in YAP-deficient hearts, we cannot distinguish which is responsible for the attenuated LVW/TL in YAP-CHKO mice after TAC. Both may contribute to the overall cardiac hypertrophy induced during the acute phase of PO, and further experimentation is needed to elucidate the mechanism driving this adaptive response.

YAP CHKO mice that we generated with αMHC-Cre mice exhibit similar cardiac phenotype as WT mice in terms of the number and cell size of CMs, CM apoptosis, and fibrosis (5). LVW/TL, left ventricular ejection fraction, or %FS also did not differ significantly between heterozygous KO and WT mice at 8 weeks (5). Thus, it is likely that the depressed cardiac function observed in YAP-CHKO after TAC occurs due to the insufficient level of YAP during PO. However, it would be difficult to completely rule out that postnatal development with depressed YAP activity leads to subtle alterations in CM phenotype that could contribute to the increased pathological susceptibility following TAC challenge.

Role of YAP in adaptive CM hypertrophy

Cardiac hypertrophy increases the number of contractile units and wall thickness, thereby reducing ventricular wall stress in the presence of hemodynamic stress and providing a benefit to the heart. Eventually, however, this response ceases to be adaptive, and heart failure develops (3). An important question is whether the hypertrophy mediated by YAP is indeed adaptive. Down-regulation of YAP blunted the extent of cardiac hypertrophy during PO, while augmenting LV wall stress, CM apoptosis, and cardiac dysfunction. This suggests that endogenous YAP plays an important role in mediating adaptive hypertrophy and protecting the heart against PO. Why, then, is YAP-mediated cardiac hypertrophy adaptive? We have shown previously that homozygous deletion of cardiac YAP results in a rapidly developing dilated cardiomyopathy, heart failure, and death by 12 weeks of age (5). Furthermore, disruption of endogenous cardiac YAP led to impaired CM survival during chronic MI and ischemia/reperfusion (5, 40). YAP is highly protective against CM death in the adult mammalian heart (17). In addition, the effect of YAP upon glycolysis (41) and angiogenesis (42) may confer an adaptive quality to YAP-induced CM growth.

How does YAP promote compensatory cardiac hypertrophy?

YAP acts as a transcription cofactor and both positively and negatively affects the function of downstream transcription factors (33). The most well characterized of these are the TEAD family transcription factors, which play a major role in mediating YAP-induced cell proliferation (20). An important question is whether TEADs are involved in YAP-induced compensatory hypertrophy during the acute phase of PO. It has been shown that cardiac-specific overexpression of TEAD1 induced CM proliferation with decreases in CM size and cardiac function (43). In that study, the authors found that stimulation of CM proliferation inhibits signaling mechanisms of cardiac hypertrophy (43). Thus, it is unlikely that the YAP–TEAD pathway mediates cardiac hypertrophy during the acute phase of PO. Further investigation, including TEAD loss-of-function studies and identification of YAP targets through ChIP sequencing during the acute phase of PO, is necessary to address this issue.

To date, several mechanisms by which YAP promotes cell survival have been identified. YAP enhances expression of antioxidant genes, including MnSOD and catalase, through activation of the FoxO family of transcription factors (40). YAP also promotes expression of Nrf2 through Pitx2 (44). We have shown previously that YAP-mediated up-regulation of miR-206 mediates hypertrophy, proliferation, and survival of CMs by down-regulating FoxP1 (45). In addition, YAP also controls the expression of Akt in CMs (5). In this study, we show that YAP regulates the activity of Akt, potentially through the down-regulation of PTEN, a negative regulator of PI3K/Akt signaling. Because Akt promotes cardiac hypertrophy (27), it is possible that Akt mediates YAP-induced compensatory hypertrophy during PO (Fig. S5).

YAP acts as a mechanosensor to mediate cardiac hypertrophy

Our results clearly show that the development of cardiac hypertrophy in response to PO is YAP-dependent. Mechanical stress occurs during pathological conditions such as volume and/or pressure overload, resulting in remodeling and altered geometry of the heart (46, 47). There is increasing evidence to suggest that the activity of YAP is regulated by mechanical forces and the actin cytoskeleton (9, 10, 48, 49). In addition, a recent study demonstrated that YAP activity is modulated by the dystrophin glycoprotein complex in CMs (50). These findings suggest that YAP may act as a mechanosensor in CMs. RhoA acts as a transducer of mechanical stress in CMs through its interaction with focal adhesions and the actin cytoskeleton and mediates downstream signaling that controls gene expression (12). We now show that RhoA is activated in the heart in response to PO and that RhoA is necessary and sufficient for

stretch- and agonist-induced activation of YAP in CMs (Fig. 7). Thus, it is likely that YAP activation during the early phase of TAC is RhoA-dependent, although the precise mechanism remains to be elucidated. Interestingly, the nuclear accumulation and stabilization of YAP after 1 week of TAC are accompanied by decreases in Ser-127 and Ser-397 phosphorylation despite the absence of change in Lats2 activation. Because RhoA regulates the activity of both kinases and phosphatases, including Rho kinase and myosin light chain phosphatase, it will be interesting to examine the potential role of the RhoA-associated kinases/phosphatases in the regulation of YAP phosphorylation during PO.

In summary, we demonstrate that endogenous YAP is activated in the heart during the acute phase of PO, as well as in CMs through a RhoA-dependent mechanism. Heterozygous deletion of CM YAP resulted in blunted cardiac hypertrophy with increased LV dilation, apoptosis, fibrosis, and dysfunction after TAC. These results indicate that endogenous YAP mediates an adaptive hypertrophic response during acute PO that serves to alleviate wall stress, protect CMs, and slow the transition to heart failure. This study highlights the beneficial role of CM YAP during acute PO and points to YAP as a potential therapeutic target for hypertension.

Experimental procedures

Animals

Generation of transgenic mice harboring a floxed Yap1 allele (C57BL/6 background) and α-MHC Cre recombinase transgenic mice (C57BL/6 background) has been previously reported (51). All animal protocols were approved by the Institutional Animal Care and Use Committee of Rutgers New Jersey Medical School.

TAC

The methods used to impose PO in mice have been described (39). Mice were anesthetized with a mixture of ketamine (0.065 mg/g), xylazine (0.013 mg/g), and acepromazine (0.002 mg/g) and mechanically ventilated. The left side of the chest was opened at the second intercostal space. Aortic constriction was performed by ligation of the transverse thoracic aorta between the innominate artery and the left common carotid artery with a 28-gauge needle using a 7-0 braided polyester suture. Sham operation was performed without constricting the aorta. To measure arterial pressure gradients, high-fidelity micromanometer catheters (1.4 French; Millar Instruments Inc.) were used.

Echocardiography

Mice were anesthetized using 12 μl/g body weight of 2.5% Avertin (Sigma), and echocardiography was performed using ultrasonography (Acuson Sequoia C256; Siemens Medical Solutions). A 13 MHz linear ultrasound transducer was used (39).

Primary CM isolation and culture

Ventricular CMs were prepared from 1-day-old Crl:(W1) BR Wistar rats (Charles River Laboratories). A CM-rich fraction was obtained by centrifugation through a discontinuous Percoll gradient. Cells were cultured in a complete medium containing Dulbecco's modified Eagle's medium/F-12 supplemented with 5% horse serum, 4 μg/ml transferrin, 0.7 ng/ml sodium selenite (Invitrogen), 2 g/liter BSA (fraction V), 3 mM pyruvic acid, 15 mM HEPES, 100 μM ascorbic acid, 100 μg/ml ampicillin, 5 μg/ml linoleic acid, and 100 μM 5-bromo-2′-deoxyuridine (Sigma). C3 toxin was purchased from Cytoskeleton, Inc. Sphingosine 1-phosphate was purchased from Avanti Polar Lipids.

Isolation and culture of adult mouse CMs

Isolation and culture of adult mouse CMs were conducted according to the protocol described in Ackers-Johnson *et al.* (52). This method utilizes direct needle perfusion of LV *ex vivo*, which allows isolation, separation, and culture of adult mouse CMs. These myocytes were used for immunostaining and immunoblotting with or without culture. Some myocytes were subjected to transduction with adenovirus vectors, and experiments were conducted 48 h after transduction.

Adenoviral constructs

Activated L63RhoA adenovirus and LacZ control adenovirus were generated as described previously (38).

Application of mechanical stretching

CMs were stretched using the Flexercell-4000 system (Flexcell International Corporation), using a modification of the system. Plates were pre-coated with collagen. Cyclical stretching of 1 Hz and 15% elongation was applied for 1 h. Control CMs were cultured on identical Flexerwell plates and maintained without mechanical stretch. Following the stretch periods, the cells were washed twice with PBS and used for cellular fraction protein analysis.

Immunoblotting

Heart homogenates or CM lysates were prepared in RIPA lysis buffer containing 50 mM Tris (pH 7.5), 150 mM NaCl, 1% IGEPAL CA-630 (Sigma), 0.1% SDS, 0.5% deoxycholic acid, 10 mM $Na_4P_2O_7$, 5 mM EDTA, 0.1 mM Na_3VO_4, 1 mM NaF, 0.5 mM 4-(2-aminoethyl)benzenesulfonyl fluoride hydrochloride, 0.5 μg/ml aprotinin, and 0.5 μg/ml leupeptin. Equal amounts of protein (5–10 μg, BCA quantification) were subjected to 10–15% SDS-PAGE. After proteins were transferred to a polyvinylidene difluoride membrane, immunoblots were probed with the indicated antibodies.

RhoA activation assay

GTP-bound RhoA in ventricular lysate was measured by pulldown according to manufacturer's instructions (Millipore Sigma).

Antibodies

Antibodies used for immunoblots were purchased from the indicated companies: p-Akt (Thr-308) (1:2,000 dilution, no. 9275), Akt (1:2,000 dilution, no. 9272), GAPDH (1:5,000 dilution, no. 2118), histone H3 (1:500 dilution, no. 9715), lamin A/C (1:5,000 dilution, no. 4777), p-Mst1 (Thr-183) (1:1,000 dilution,

no. 3681), p-YAP (Ser-127) (1:1,000 dilution, no. 4911), p-YAP (Ser-397) (1:1,000 dilution, no. 13619), YAP (1:2,000 dilution, no. 14074), and p-Lats2 (Ser-909 and Thr-1079) (1:1,000 dilution, nos. 9157 and 8654) (Cell Signaling Technology); α-tubulin (1:10,000 dilution, no. T6074) (Sigma); Mst1 (1:2,000 dilution, no. 611052) (BD Biosciences); Lats2 (1:1,000 dilution, nos. ab54073 and A300-479A) (Abcam and Bethyl Laboratories, respectively); Ki-67 (1:500 dilution, no. 9129) (Cell Signaling Technology); RhoA (1:1,000 dilution, no. ARH03-A) (Cytoskeleton); RhoGDI (1:5,000 dilution, no. 2564), GSK-3 (1:1,000 dilution, no. 5676), p-GSK-3 (Ser-21/9) (1:1,000 dilution, no. 9327), PTEN (1:1,000, no. 9188), and β-actinin (1:5,000, no. 8457) (Cell Signaling Technology).

Subcellular fractionation

The nuclear and cytosolic fractions were prepared with NE-PER Nuclear and Cytoplasmic Extraction Reagents (Pierce). After isolating cytosolic and nuclear fractions, immunoblotting was conducted.

Quantitative RT-PCR

RNA was isolated from the mouse hearts; cDNA was generated, and quantitative RT-PCR was performed as described previously (36). Primers used were as follows: Anf, sense (5′-ATACAGTGCGGTGTCCAACA-3′) and antisense (5′-CGAGAGCACCTCCATCTCTC-3′); Yap, sense (5′-AGGAGAGACTGCGGTTGAAA-3′) and antisense (5′-CCTGAGACATCCAGGAGAA-3′); Ctgf, sense (5′-CAAAGCAGCTGCAAATACCA-3′) and antisense (5′-GGCCAAATGTGTCTTCCAGT-3′); Ankrd1 sense (5′-TTGTGAAGGAGCCAGAACCT-3′) and antisense (5′-CGCCAAGTGTCCTTCTAAGC-3′).

Immunostaining

Neonatal rat CMs grown on chamber slides (Lab-Tek) were washed three times with PBS. The cells were fixed with 4% paraformaldehyde and washed four times with PBS containing 0.1% Triton X-100. The cells were boiled for 10 min with a pressure cooker to allow better exposure of the antigen to the antibody. The cells were then blocked with PBS containing 5% normal goat serum for 60 min and stained with antibodies as indicated.

Histological analyses

The LV accompanied by the septum was cut into base, middle portion, and apex, fixed with 10% formalin, embedded in paraffin, and sectioned at 6-μm thickness. The sections were incubated in 3% H_2O_2 in PBS to prevent endogenous peroxidation and blocked with 5% BSA in PBS. CM cross-sectional area was measured from images captured of sections stained with anti-wheat germ agglutinin antibody as described previously (39). The outlines of 200 CMs were traced in each section. Interstitial fibrosis was evaluated by Masson's Trichrome staining. Heart sections were stained with anti-YAP1 rabbit polyclonal antibody (Cell Signaling), anti-troponin-T mouse mAb (Neomarkers), Alexa Fluor 488–conjugated goat anti-rabbit IgG (Invitrogen), Alexa Fluor 594–conjugated goat anti-mouse IgG (Invitrogen), and Vectashield mounting medium with DAPI (Vector Laboratories). Analyses were performed using fluorescence microscopy (Ti, Nikon).

Apoptosis assays

TUNEL staining was conducted as described (35). Deparaffinized sections were incubated with proteinase K, and DNA fragments were labeled with fluorescein-conjugated dUTP using terminal deoxynucleotidyltransferase (Roche Applied Science). Nuclear density was determined by manual counting of DAPI-stained nuclei in 7–10 fields for each animal using a $\times$20 objective.

Statistics

All values are expressed as the mean $\pm$ S.D. Statistical analyses were performed by either t test or analysis of variance and the Tukey post-test procedure, with $p < 0.05$ considered significant.

Author contributions—J. B., D. P. D. R., S. I., A. S., and S. M. data curation; J. B., D. P. D. R., P. Z., S. I., A. S., W. M., and S. M. investigation; J. B. writing-original draft; J. B., D. P. D. R., J. H. B., and J. S. writing-review and editing; D. P. D. R. and P. Z. formal analysis; D. P. D. R., J. H. B., and J. S. supervision; D. P. D. R., J. H. B., and J. S. funding acquisition; J. S. conceptualization.

Acknowledgment—We thank Daniela Zablocki for critical reading of the manuscript.

References

1. Benjamin, E. J., Virani, S. S., Callaway, C. W., Chamberlain, A. M., Chang, A. R., Cheng, S., Chiuve, S. E., Cushman, M., Delling, F. N., Deo, R., de Ferranti, S. D., Ferguson, J. F., Fornage, M., Gillespie, C., Isasi, C. R., *et al.* (2018) Heart Disease and Stroke Statistics–2018 Update: a report from the American Heart Association. *Circulation* **137,** e67-e492 Medline
2. Nakamura, M., and Sadoshima, J. (2018) Mechanisms of physiological and pathological cardiac hypertrophy. *Nat. Rev. Cardiol.* **15,** 387–407 CrossRef Medline
3. Ruwhof, C., and van der Laarse, A. (2000) Mechanical stress-induced cardiac hypertrophy: mechanisms and signal transduction pathways. *Cardiovasc. Res.* **47,** 23–37 CrossRef
4. Shirakabe, A., Zhai, P., Ikeda, Y., Saito, T., Maejima, Y., Hsu, C. P., Nomura, M., Egashira, K., Levine, B., and Sadoshima, J. (2016) Drp1-dependent mitochondrial autophagy plays a protective role against pressure overload-induced mitochondrial dysfunction and heart failure. *Circulation* **133,** 1249–1263 CrossRef Medline
5. Del Re, D. P., Yang, Y., Nakano, N., Cho, J., Zhai, P., Yamamoto, T., Zhang, N., Yabuta, N., Nojima, H., Pan, D., and Sadoshima, J. (2013) Yes-associated protein isoform 1 (Yap1) promotes cardiomyocyte survival and growth to protect against myocardial ischemic injury. *J. Biol. Chem.* **288,** 3977–3988 CrossRef Medline
6. Hill, J. A., and Olson, E. N. (2008) Cardiac plasticity. *N. Engl. J. Med.* **358,** 1370–1380 CrossRef Medline
7. Heineke, J., and Molkentin, J. D. (2006) Regulation of cardiac hypertrophy by intracellular signalling pathways. *Nat. Rev. Mol. Cell Biol.* **7,** 589–600 CrossRef Medline
8. Lorell, B. H., and Carabello, B. A. (2000) Left ventricular hypertrophy: pathogenesis, detection, and prognosis. *Circulation* **102,** 470–479 CrossRef Medline
9. Dupont, S., Morsut, L., Aragona, M., Enzo, E., Giulitti, S., Cordenonsi, M., Zanconato, F., Le Digabel, J., Forcato, M., Bicciato, S., Elvassore, N., and Piccolo, S. (2011) Role of YAP/TAZ in mechanotransduction. *Nature* **474,** 179–183 CrossRef Medline

10. Aragona, M., Panciera, T., Manfrin, A., Giulitti, S., Michielin, F., Elvassore, N., Dupont, S., and Piccolo, S. (2013) A mechanical checkpoint controls multicellular growth through YAP/TAZ regulation by actin-processing factors. *Cell* **154,** 1047–1059 CrossRef Medline
11. Wada, K., Itoga, K., Okano, T., Yonemura, S., and Sasaki, H. (2011) Hippo pathway regulation by cell morphology and stress fibers. *Development* **138,** 3907–3914 CrossRef Medline
12. Brown, J. H., Del Re, D. P., and Sussman, M. A. (2006) The Rac and Rho hall of fame: a decade of hypertrophic signaling hits. *Circ. Res.* **98,** 730–742 CrossRef Medline
13. Mo, J. S., Yu, F. X., Gong, R., Brown, J. H., and Guan, K. L. (2012) Regulation of the Hippo-YAP pathway by protease-activated receptors (PARs). *Genes Dev.* **26,** 2138–2143 CrossRef Medline
14. Yu, F. X., Zhao, B., Panupinthu, N., Jewell, J. L., Lian, I., Wang, L. H., Zhao, J., Yuan, H., Tumaneng, K., Li, H., Fu, X. D., Mills, G. B., and Guan, K. L. (2012) Regulation of the Hippo-YAP pathway by G-protein-coupled receptor signaling. *Cell* **150,** 780–791 CrossRef Medline
15. Xiang, S. Y., Vanhoutte, D., Del Re, D. P., Purcell, N. H., Ling, H., Banerjee, I., Bossuyt, J., Lang, R. A., Zheng, Y., Matkovich, S. J., Miyamoto, S., Molkentin, J. D., Dorn, G. W., 2nd., and Brown, J. H. (2011) RhoA protects the mouse heart against ischemia/reperfusion injury. *J. Clin. Invest.* **121,** 3269–3276 CrossRef Medline
16. Del Re, D. P., Miyamoto, S., and Brown, J. H. (2008) Focal adhesion kinase as a RhoA-activable signaling scaffold mediating Akt activation and cardiomyocyte protection. *J. Biol. Chem.* **283,** 35622–35629 CrossRef Medline
17. Wackerhage, H., Del Re, D. P., Judson, R. N., Sudol, M., and Sadoshima, J. (2014) The Hippo signal transduction network in skeletal and cardiac muscle. *Sci. Signal.* **7,** re4 CrossRef Medline
18. He, M., Zhou, Z., Shah, A. A., Hong, Y., Chen, Q., and Wan, Y. (2016) New insights into posttranslational modifications of Hippo pathway in carcinogenesis and therapeutics. *Cell Div.* **11,** 4 CrossRef Medline
19. Ikeda, S., Mizushima, W., Sciarretta, S., Abdellatif, M., Zhai, P., Mukai, R., Fefelova, N., Oka, S. I., Nakamura, M., Del Re, D. P., Farrance, I., Park, J. Y., Tian, B., Xie, L. H., Kumar, M., *et al.* (2019) Hippo deficiency leads to cardiac dysfunction accompanied by cardiomyocyte dedifferentiation during pressure overload. *Circ. Res.* **124,** 292–305 CrossRef Medline
20. Zhao, B., Ye, X., Yu, J., Li, L., Li, W., Li, S., Yu, J., Lin, J. D., Wang, C. Y., Chinnaiyan, A. M., Lai, Z. C., and Guan, K. L. (2008) TEAD mediates YAP-dependent gene induction and growth control. *Genes Dev.* **22,** 1962–1971 CrossRef Medline
21. Li, C., Srivastava, R. K., Elmets, C. A., Afaq, F., and Athar, M. (2013) Arsenic-induced cutaneous hyperplastic lesions are associated with the dysregulation of Yap, a Hippo signaling-related protein. *Biochem. Biophys. Res. Commun.* **438,** 607–612 CrossRef Medline
22. von Gise, A., Lin, Z., Schlegelmilch, K., Honor, L. B., Pan, G. M., Buck, J. N., Ma, Q., Ishiwata, T., Zhou, B., Camargo, F. D., and Pu, W. T. (2012) YAP1, the nuclear target of Hippo signaling, stimulates heart growth through cardiomyocyte proliferation but not hypertrophy. *Proc. Natl. Acad. Sci. U.S.A.* **109,** 2394–2399 CrossRef Medline
23. Xin, M., Kim, Y., Sutherland, L. B., Murakami, M., Qi, X., McAnally, J., Porrello, E. R., Mahmoud, A. I., Tan, W., Shelton, J. M., Richardson, J. A., Sadek, H. A., Bassel-Duby, R., and Olson, E. N. (2013) Hippo pathway effector Yap promotes cardiac regeneration. *Proc. Natl. Acad. Sci. U.S.A.* **110,** 13839–13844 CrossRef Medline
24. Beltrami, A. P., Urbanek, K., Kajstura, J., Yan, S. M., Finato, N., Bussani, R., Nadal-Ginard, B., Silvestri, F., Leri, A., Beltrami, C. A., and Anversa, P. (2001) Evidence that human cardiac myocytes divide after myocardial infarction. *N. Engl. J. Med.* **344,** 1750–1757 CrossRef Medline
25. Lauriol, J., Keith, K., Jaffré, F., Couvillon, A., Saci, A., Goonasekera, S. A., McCarthy, J. R., Kessinger, C. W., Wang, J., Ke, Q., Kang, P. M., Molkentin, J. D., Carpenter, C., and Kontaridis, M. I. (2014) RhoA signaling in cardiomyocytes protects against stress-induced heart failure but facilitates cardiac fibrosis. *Sci. Signal.* **7,** ra100 CrossRef Medline
26. Sadoshima, J., Jahn, L., Takahashi, T., Kulik, T. J., and Izumo, S. (1992) Molecular characterization of the stretch-induced adaptation of cultured cardiac cells. An *in vitro* model of load-induced cardiac hypertrophy. *J. Biol. Chem.* **267,** 10551–10560 Medline
27. Condorelli, G., Drusco, A., Stassi, G., Bellacosa, A., Roncarati, R., Iaccarino, G., Russo, M. A., Gu, Y., Dalton, N., Chung, C., Latronico, M. V., Napoli, C., Sadoshima, J., Croce, C. M., and Ross, J., Jr. (2002) Akt induces enhanced myocardial contractility and cell size *in vivo* in transgenic mice. *Proc. Natl. Acad. Sci. U.S.A.* **99,** 12333–12338 CrossRef Medline
28. Shioi, T., McMullen, J. R., Kang, P. M., Douglas, P. S., Obata, T., Franke, T. F., Cantley, L. C., and Izumo, S. (2002) Akt/protein kinase B promotes organ growth in transgenic mice. *Mol. Cell. Biol.* **22,** 2799–2809 CrossRef Medline
29. Matsui, T., Li, L., Wu, J. C., Cook, S. A., Nagoshi, T., Picard, M. H., Liao, R., and Rosenzweig, A. (2002) Phenotypic spectrum caused by transgenic overexpression of activated Akt in the heart. *J. Biol. Chem.* **277,** 22896–22901 CrossRef Medline
30. Mocanu, M. M., and Yellon, D. M. (2007) PTEN, the Achilles' heel of myocardial ischaemia/reperfusion injury? *Br. J. Pharmacol.* **150,** 833–838 CrossRef Medline
31. Tumaneng, K., Schlegelmilch, K., Russell, R. C., Yimlamai, D., Basnet, H., Mahadevan, N., Fitamant, J., Bardeesy, N., Camargo, F. D., and Guan, K. L. (2012) YAP mediates crosstalk between the Hippo and PI(3)K-TOR pathways by suppressing PTEN via miR-29. *Nat. Cell Biol.* **14,** 1322–1329 CrossRef Medline
32. Lin, Z., von Gise, A., Zhou, P., Gu, F., Ma, Q., Jiang, J., Yau, A. L., Buck, J. N., Gouin, K. A., van Gorp, P. R., Zhou, B., Chen, J., Seidman, J. G., Wang, D. Z., and Pu, W. T. (2014) Cardiac-specific YAP activation improves cardiac function and survival in an experimental murine myocardial infarction model. *Circ. Res.* **115,** 354–363 CrossRef Medline
33. Yu, F. X., Zhao, B., and Guan, K. L. (2015) Hippo pathway in organ size control, tissue homeostasis, and cancer. *Cell* **163,** 811–828 CrossRef Medline
34. Maillet, M., van Berlo, J. H., and Molkentin, J. D. (2013) Molecular basis of physiological heart growth: fundamental concepts and new players. *Nat. Rev. Mol. Cell Biol.* **14,** 38–48 CrossRef Medline
35. Yamamoto, S., Yang, G., Zablocki, D., Liu, J., Hong, C., Kim, S. J., Soler, S., Odashima, M., Thaisz, J., Yehia, G., Molina, C. A., Yatani, A., Vatner, D. E., Vatner, S. F., and Sadoshima, J. (2003) Activation of Mst1 causes dilated cardiomyopathy by stimulating apoptosis without compensatory ventricular myocyte hypertrophy. *J. Clin. Invest.* **111,** 1463–1474 CrossRef Medline
36. Matsui, Y., Nakano, N., Shao, D., Gao, S., Luo, W., Hong, C., Zhai, P., Holle, E., Yu, X., Yabuta, N., Tao, W., Wagner, T., Nojima, H., and Sadoshima, J. (2008) Lats2 is a negative regulator of myocyte size in the heart. *Circ. Res.* **103,** 1309–1318 CrossRef Medline
37. Heallen, T., Morikawa, Y., Leach, J., Tao, G., Willerson, J. T., Johnson, R. L., and Martin, J. F. (2013) Hippo signaling impedes adult heart regeneration. *Development* **140,** 4683–4690 CrossRef Medline
38. Del Re, D. P., Miyamoto, S., and Brown, J. H. (2007) RhoA/Rho kinase up-regulate Bax to activate a mitochondrial death pathway and induce cardiomyocyte apoptosis. *J. Biol. Chem.* **282,** 8069–8078 CrossRef Medline
39. Matsuda, T., Zhai, P., Maejima, Y., Hong, C., Gao, S., Tian, B., Goto, K., Takagi, H., Tamamori-Adachi, M., Kitajima, S., and Sadoshima, J. (2008) Distinct roles of GSK-3α and GSK-3β phosphorylation in the heart under pressure overload. *Proc. Natl. Acad. Sci. U.S.A.* **105,** 20900–20905 CrossRef Medline
40. Shao, D., Zhai, P., Del Re, D. P., Sciarretta, S., Yabuta, N., Nojima, H., Lim, D. S., Pan, D., and Sadoshima, J. (2014) A functional interaction between Hippo-YAP signalling and FoxO1 mediates the oxidative stress response. *Nat. Commun.* **5,** 3315 CrossRef Medline
41. Wang, X., Ha, T., Liu, L., Hu, Y., Kao, R., Kalbfleisch, J., Williams, D., and Li, C. (2018) TLR3 mediates repair and regeneration of damaged neonatal heart through glycolysis dependent YAP1 regulated miR-152 expression. *Cell Death Differ.* **25,** 966–982 CrossRef Medline
42. Astone, M., Lai, J. K. H., Dupont, S., Stainier, D. Y. R., Argenton, F., and Vettori, A. (2018) Zebrafish mutants and TEAD reporters reveal essential functions for Yap and Taz in posterior cardinal vein development. *Sci. Rep.* **8,** 10189 CrossRef Medline
43. Tsika, R. W., Ma, L., Kehat, I., Schramm, C., Simmer, G., Morgan, B., Fine, D. M., Hanft, L. M., McDonald, K. S., Molkentin, J. D., Krenz, M., Yang, S.,

and Ji, J. (2010) TEAD-1 overexpression in the mouse heart promotes an age-dependent heart dysfunction. *J. Biol. Chem.* **285,** 13721–13735 CrossRef Medline

44. Tao, G., Kahr, P. C., Morikawa, Y., Zhang, M., Rahmani, M., Heallen, T. R., Li, L., Sun, Z., Olson, E. N., Amendt, B. A., and Martin, J. F. (2016) Pitx2 promotes heart repair by activating the antioxidant response after cardiac injury. *Nature* **534,** 119–123 CrossRef Medline
45. Yang, Y., Del Re, D. P., Nakano, N., Sciarretta, S., Zhai, P., Park, J., Sayed, D., Shirakabe, A., Matsushima, S., Park, Y., Tian, B., Abdellatif, M., and Sadoshima, J. (2015) miR-206 mediates YAP-induced cardiac hypertrophy and survival. *Circ. Res.* **117,** 891–904 CrossRef Medline
46. Sadoshima, J., and Izumo, S. (1997) The cellular and molecular response of cardiac myocytes to mechanical stress. *Annu. Rev. Physiol.* **59,** 551–571 CrossRef Medline
47. Cohn, J. N., Ferrari, R., and Sharpe, N. (2000) Cardiac remodeling–concepts and clinical implications: a consensus paper from an international forum on cardiac remodeling. Behalf of an international forum on cardiac remodeling. *J. Am. Coll. Cardiol.* **35,** 569–582 CrossRef Medline
48. Reddy, P., Deguchi, M., Cheng, Y., and Hsueh, A. J. (2013) Actin cytoskeleton regulates Hippo signaling. *PLoS ONE* **8,** e73763 CrossRef Medline
49. Ohgushi, M., Minaguchi, M., and Sasai, Y. (2015) Rho-signaling-directed YAP/TAZ activity underlies the long-term survival and expansion of human embryonic stem cells. *Cell Stem Cell* **17,** 448–461 CrossRef Medline
50. Morikawa, Y., Heallen, T., Leach, J., Xiao, Y., and Martin, J. F. (2017) Dystrophin glycoprotein complex sequesters Yap to inhibit cardiomyocyte proliferation. *Nature* **547,** 227–231 CrossRef Medline
51. Zhang, N., Bai, H., David, K. K., Dong, J., Zheng, Y., Cai, J., Giovannini, M., Liu, P., Anders, R. A., and Pan, D. (2010) The Merlin/NF2 tumor suppressor functions through the YAP oncoprotein to regulate tissue homeostasis in mammals. *Dev. Cell* **19,** 27–38 CrossRef Medline
52. Ackers-Johnson, M., Li, P. Y., Holmes, A. P., O'Brien, S. M., Pavlovic, D., and Foo, R. S. (2016) A simplified, Langendorff-free method for concomitant isolation of viable cardiac myocytes and nonmyocytes from the adult mouse heart. *Circ. Res.* **119,** 909–920 CrossRef Medline